Interaction-driven Spontaneous Ferromagnetic Insulating States with an Odd Chern Number: supplementary information

Peizhi Mai[1], Edwin W. Huang[1], Jiachen Yu[2,3], Benjamin E. Feldman[3,4,5], Philip W. Phillips[1,†]
[1]Department of Physics and Institute of Condensed Matter Theory,
University of Illinois at Urbana-Champaign, Urbana, IL 61801, USA
[2]Department of Applied Physics, Stanford University, Stanford, CA 94305, USA
[3]Geballe Laboratory of Advanced Materials, Stanford, CA 94305, USA
[4]Department of Physics, Stanford University, Stanford, CA 94305, USA and
[5]Stanford Institute for Materials and Energy Sciences,
SLAC National Accelerator Laboratory, Menlo Park, CA 94025, USA

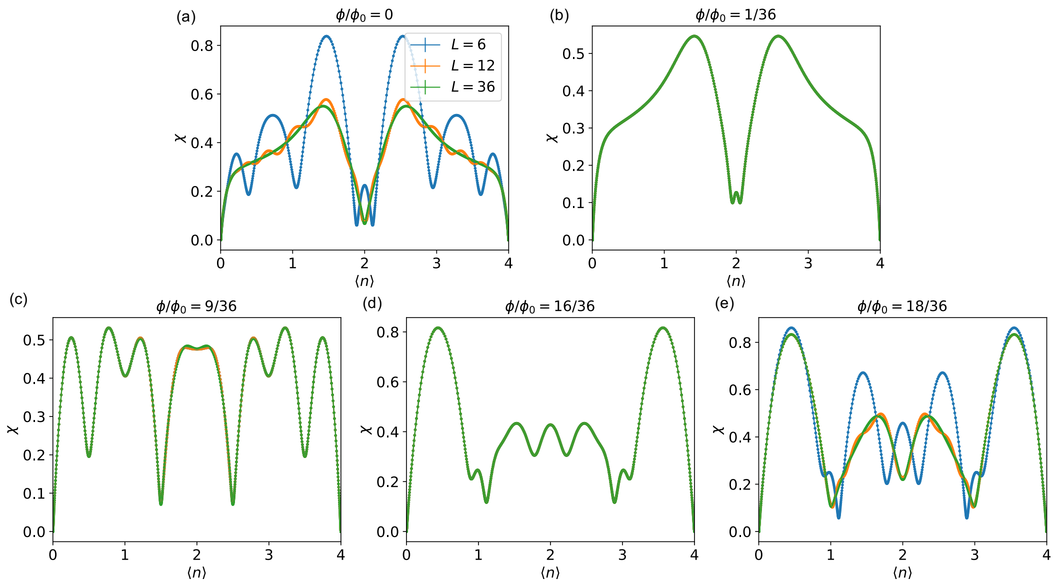

FIG. S1. Non-interacting compressibility for several system sizes ($L = 6, 12, 36$) under different fixed magnetic fluxes (a) $\phi/\phi_0 = 0$, (b) $\phi/\phi_0 = 1/36$, (c) $\phi/\phi_0 = 9/36$, (d) $\phi/\phi_0 = 16/36$, (e) $\phi/\phi_0 = 18/36$. The inverse temperature is $\beta = 8$.

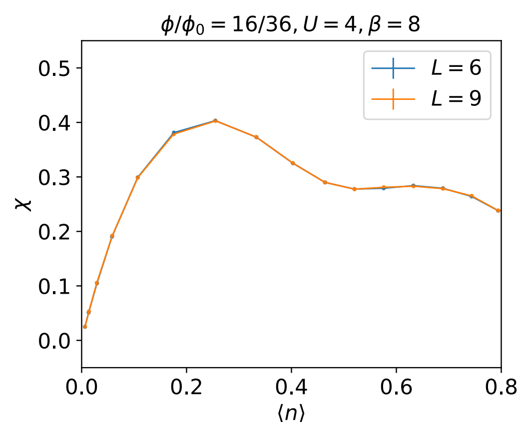

FIG. S2. The incompressible region in the compressibility caused by the interaction for different cluster sizes $N_{\text{site}} = 6 \times 6 \times 2$ and $N_{\text{site}} = 9 \times 9 \times 2$. The fixed parameters are $\beta = 8/t$, $U = 4t$, $\phi/\phi_0 = 16/36$. Both curves collapse, indicating the incompressible state is not related to finite-size effects.

We show the finite-size effect on the non-interacting system in Fig. S1. For $\phi/\phi_0 = 0, 0.5$, the compressibility endures strong finite-size effects as evidenced by the unphysical valleys which become flattened as the system size increases. With (even the smallest) magnetic field, there is barely any finite-size effect because the lines collapse among different system sizes, except at $\phi/\phi_0 = 0.5$. This explains the "additional" state shown in $\phi/\phi_0 = 0, 0.5$ of Fig. 2(a-d) in the main text with and without interactions. This state is incompatible with the remaining part of the panel ($0 < \phi/\phi_0 < 0.5$). Those unphysical incompressible states disappear at a larger system size as shown in Fig.1 of the main text. In Fig. S2, we show the incompressible state in the dilute region at different lattice sizes. The results overlay as expected for $\phi/\phi_0 = 16/36$ which illustrates that this emergent incompressible state with Chern number $= 1$ is robust against increasing system size.

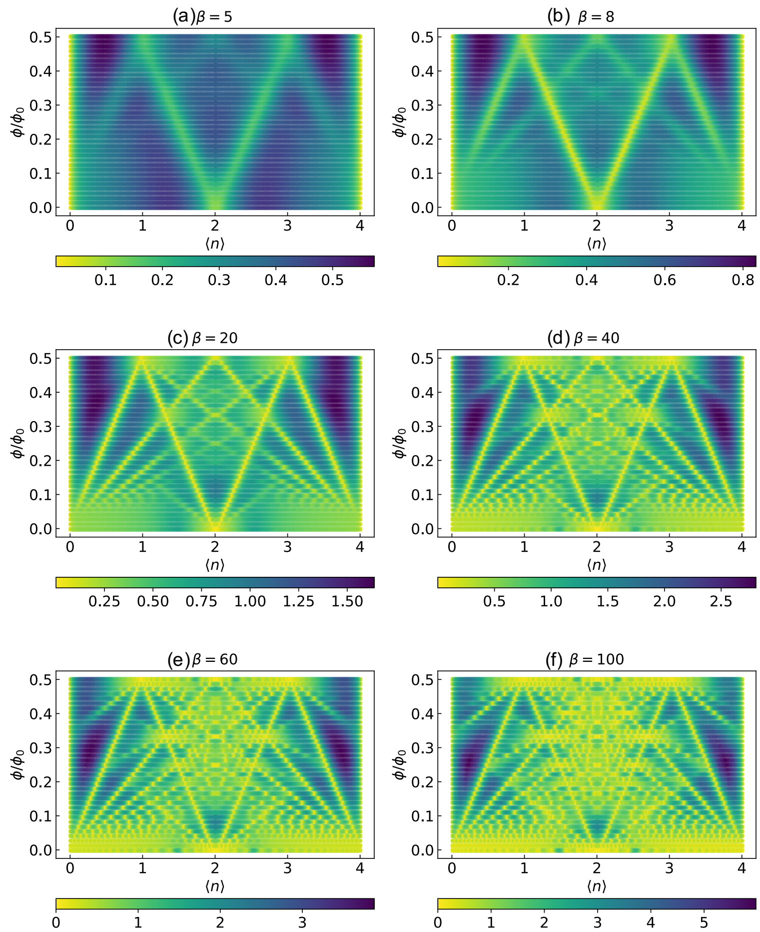

FIG. S3. Non-interacting compressibility as a function of magnetic flux and density at different temperatures (a) $\beta = 5/t$, (b) $\beta = 8/t$, (c) $\beta = 20/t$, (d) $\beta = 40/t$, (e) $\beta = 60/t$, (f) $\beta = 100/t$.

We show the non-interacting compressibility at different temperatures in Fig. S3. As the temperature decreases, we observe more straight lines (incompressible states) representing different quantum Hall states. Particularly, for $\beta \gtrsim 40/t$, incompressible Hofstadter states in the top left and right regions represented by straight lines from quarter fillings $\langle n \rangle = 1$ and $\langle n \rangle = 3$ at $\phi/\phi_0 = 0.5$. They correspond to straight lines passing through quarter-filling at ϕ/ϕ_0 and appear at $\phi/\phi_0 \geq 1/3$. These two features do not match the additional valleys we observe in Fig. 2(e) and Fig. 3 of the main text. Therefore, the new valleys in Fig. 2(e) and Fig. 3 of the main text are derived from the interactions.

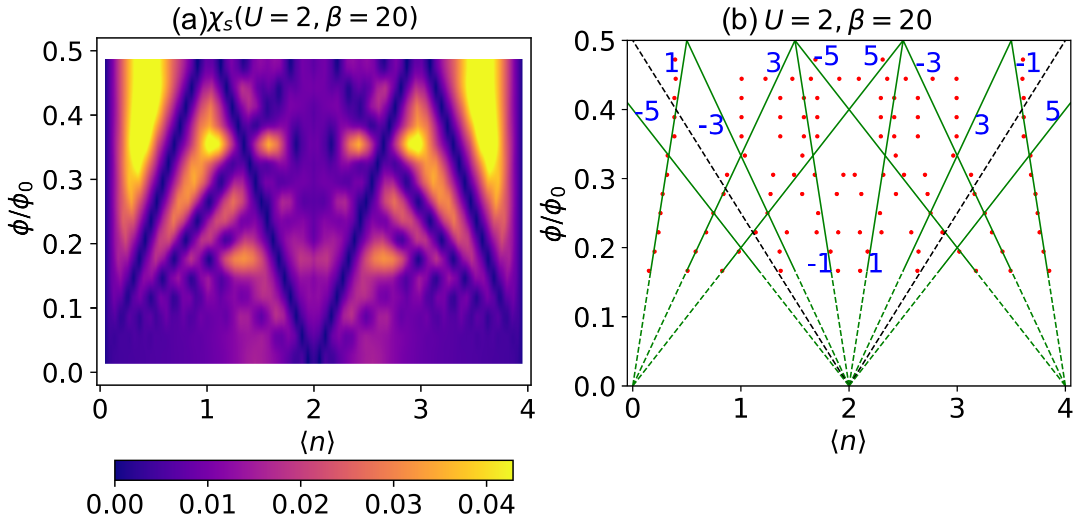

FIG. S4. Replot of Fig.2(f) and Fig.3(i) from the main text for further clarification. The additional dashed lines in panel (b) represent possible ferromagnetic states with Chern number $= \pm 4$.

We re-plot the Fig.2 (f) and Fig.3 (i) of the main text in Fig. S4 to further discuss the slight mismatch between the peak location in spin correlation and odd-integer quantum Hall ferromagnetic states. The peak height of the spin correlation decreases in the vicinity of the charge neutrality point (CNP) $\langle n \rangle = 2$, which displays a strong antiferromagnetic pattern for all magnetic fields. This makes it difficult to resolve the peak location for the spin-polarized state with Chern number ± 1 from CNP at zero field, though these local maxima indeed are enhanced by the interaction. Another factor affecting the resolution is that the interaction strength here is only $U/t = 2$. At a larger U, we expect higher peaks which would ease in pinpointing their location more accurately. In fact, the observation that a series of odd-integer ferromagnetic quantum Hall states meet at (or at least extrapolate to) the antiferromagnetic CNP point is interesting and worth further study. Another major area of mismatch is around $\langle n \rangle = 1.5$, $\phi/\phi_0 = 6 \sim 7/36$ and its particle-hole counterpart. A possible reason is that the odd-integer states with Chern number $\pm 3, 5$ are so close that they merge into a single peak at this level of resolution. It is also possible that there is a ferromagnetic state with Chern number ± 4 shown in the black dashed lines in Fig. S4(b) which cross a few red dots. If this is true, this even integer ferromagnetic state are also emergent in contrast to the non-interacting even-integer paramagnetic quantum Hall states. However, our current resolution can not confirm (or rule out) this possibility.

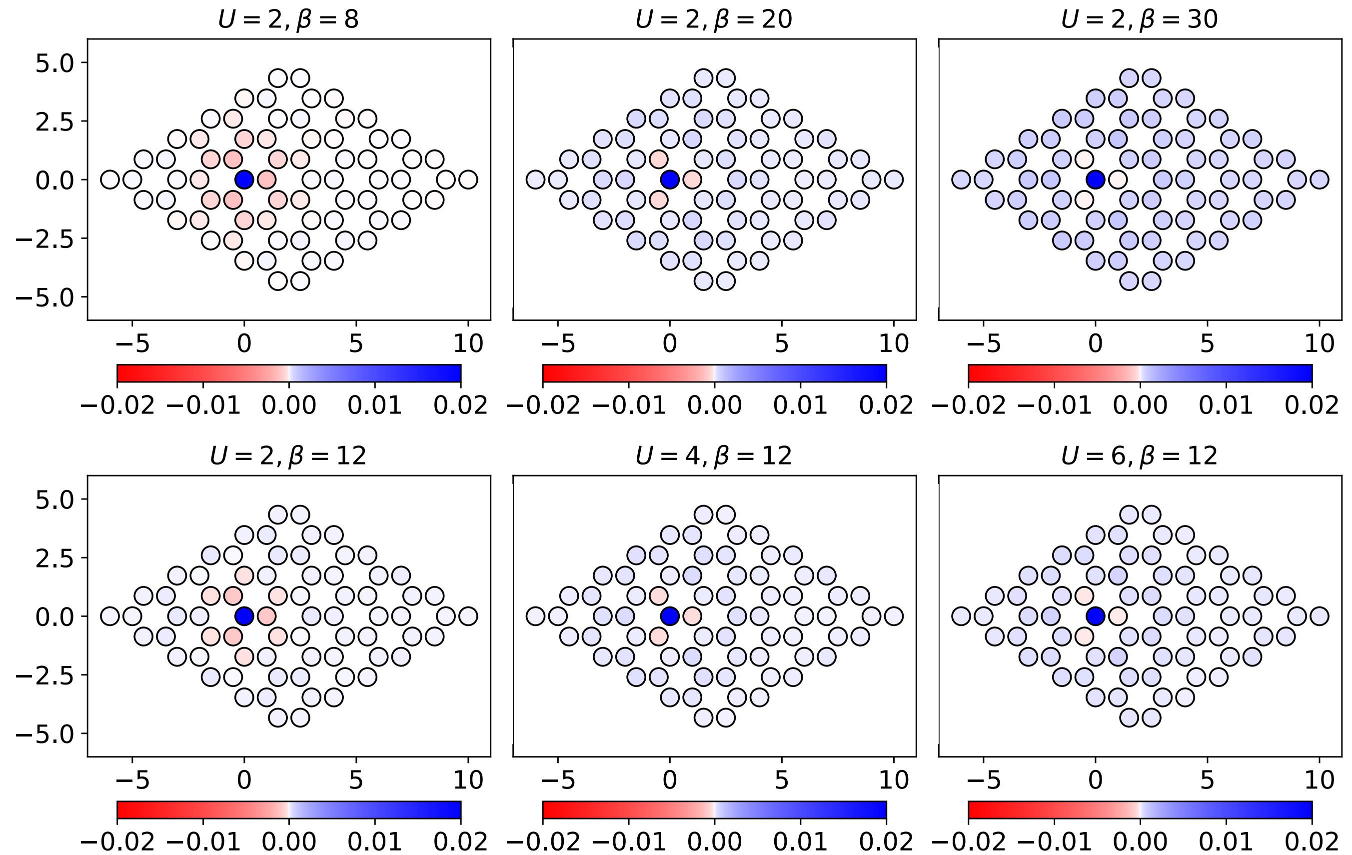

FIG. S5. Spin correlation at $\phi/\phi_0 = 12/36$ and $\langle n \rangle = 1/3$ varying temperature with $U/t = 2$ in the first row and varying U with $\beta = 12/t$ in the second row.

We show the spin correlation for $\phi/\phi_0 = 12/36$, $\langle n \rangle = 1/3$ in Fig. S5 at 1) varying temperatures with U fixed and 2) varying U with temperature fixed. As the temperature decreases or interaction increases, ferromagnetism ensues.

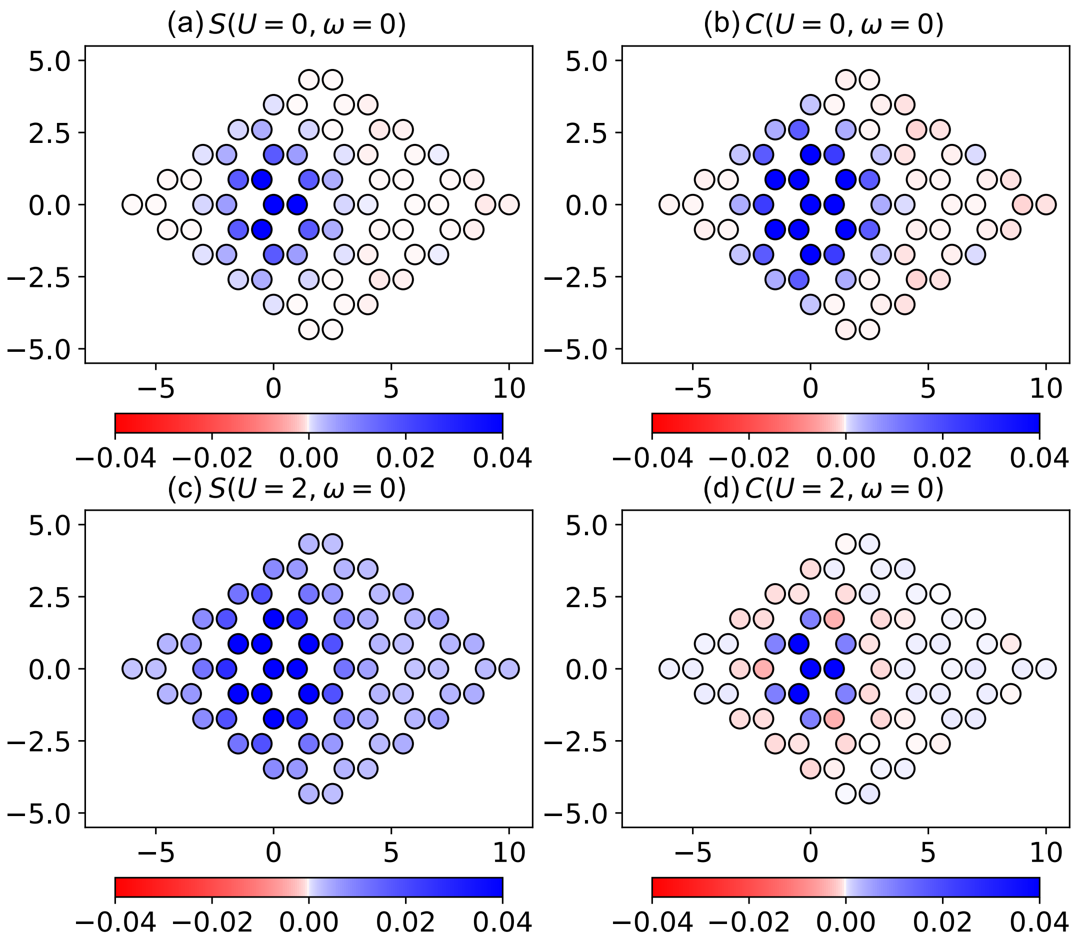

FIG. S6. Zero-frequency spin (a,c) and charge (b,d) correlation at $\phi/\phi_0 = 12/36$ and $\langle n\rangle = 1/3$ for $U/t = 0$ in the first row and $U/t = 2$ in the second row. The inverse temperature is $\beta = 20/t$ for all panels.

The zero-frequency correlation function is more sensitive for the detection of fluctuating stripe patterns at finite temperature due to the integration over imaginary time. The $\omega = 0$ correlation is defined as

$$S(\mathbf{r}, \omega = 0) = \frac{1}{N}\int_0^\beta \sum_{\mathbf{i}} \langle S^z_{\mathbf{i}+\mathbf{r}}(\tau) S^z_{\mathbf{i}}(0)\rangle d\tau. \tag{S1}$$

for the spin case, and

$$C(\mathbf{r}, \omega = 0) = \frac{1}{N}\int_0^\beta \sum_{\mathbf{i}} \left[\langle n_{\mathbf{i}+\mathbf{r}}(\tau) n_j(0)\rangle - \langle n_{\mathbf{i}+\mathbf{r}}(\tau)\rangle\langle n_{\mathbf{i}}(0)\rangle\right] d\tau. \tag{S2}$$

for the charge correlation. They are plotted in Fig. S6 at $\phi/\phi_0 = 12/36$, $\langle n\rangle = 1/3$ and $\beta = 20/t$ for $U/t = 0, 2$. In the non-interacting case, the spin pattern in panel (a) looks just the same as the charge pattern in panel (b) with the factor of $1/4$ in amplitude. After turning on the interaction, as shown in the Fig. 3 of the main text, a sharper peak develops in the spin correlation and a dip emerges in the charge correlation for this parameter set. Correspondingly, the real-space resolved spin correlation displays a ferromagnetic pattern in panel (c) and charge correlation represents a two-dimensional stripe pattern in panel (d) signaled by a blue area in the middle surrounded by a red ring region. The nature of the charge stripes deserves further study.

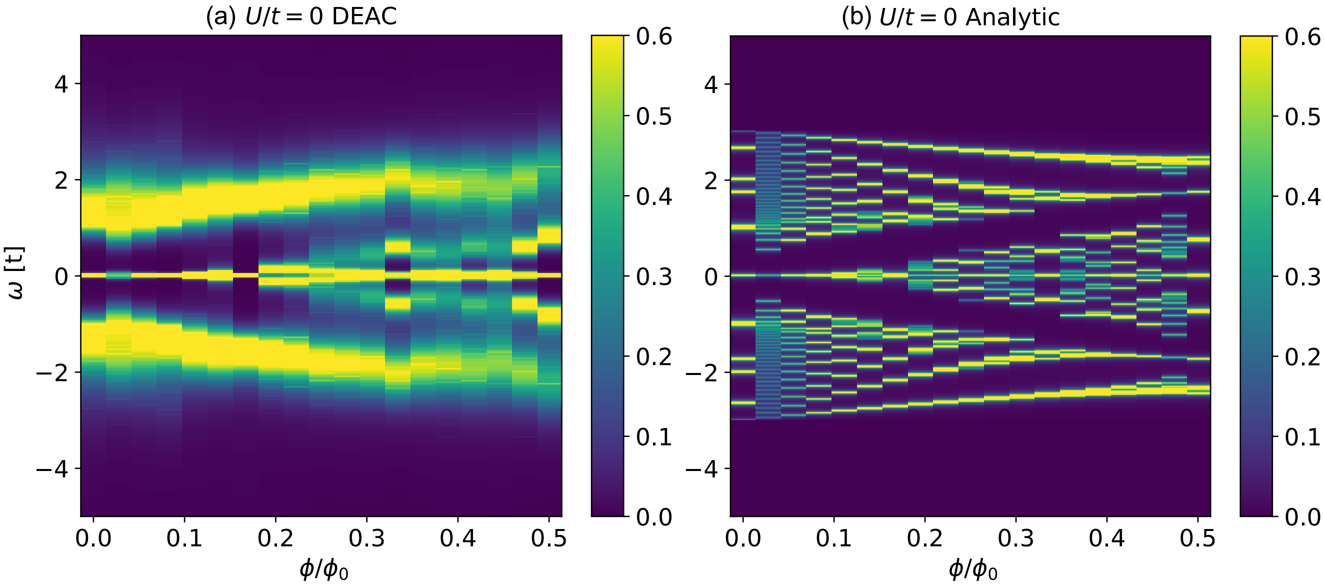

FIG. S7. The non-interacting density of states from (a) an analytical-continuation of DQMC local Green functions at $\beta = 30/t$ by DEAC and (b) an analytical calculation at zero temperature.

We show the comparison between the DEAC density of state at $\beta = 30/t$ and the analytic density of states at zero temperature in Fig. S7. Note that the analytic density of states is independent of temperature, while DEAC requires lower temperature (larger β) to improve the resolution. From the comparison, we can tell that DEAC captures the main feature of the analytic result (the primary branches and gaps) although it fails to reproduce the detailed fractal pattern.